

# Performance Study of Nitride-Based Gunn Diodes

G. Aloise, S. Vitanov, and V. Palankovski

Advanced Material and Device Analysis Group  
Inst. for Microelectronics, TU Wien, A-1040 Vienna, Austria  
aloise@iue.tuwien.ac.at

## ABSTRACT

In this work, the performance of InN and GaN Gunn diodes is assessed by means of two-dimensional mixed-mode device/circuit simulation. A proprietary hydrodynamic high-field mobility model is used, calibrated against Monte Carlo simulation data, which properly accounts for the negative differential mobility effect. Available theoretical results for GaN-based Gunn diodes are verified. The simulation results predict superior performance of GaN below 200 GHz while InN Gunn diodes show promising potential for the higher frequency range.

**Keywords:** simulation, Gunn diodes, Indium Nitride, Gallium Nitride

## 1 INTRODUCTION

Low-power microwave transmitters require nanoscale devices operated in terahertz regime. This can be achieved by using transferred-electron devices based on Gunn oscillations (Gunn oscillators). Such devices exhibit favorable characteristics, like low FM noise, which makes them suitable for applications like injection-locked oscillators and amplifiers [1]. Negative differential mobility (NDM) is a requirement for the occurrence of the Gunn effect, which has been already extensively studied in GaAs. The frequency of oscillation of a Gunn device is determined by the time taken for a Gunn domain to form and complete the transit between the cathode and anode contacts [2]. For this reason, it would be desirable to minimize the transit time of Gunn domains, in order to achieve higher frequencies. This can be realized through a higher electron drift velocity. The wide bandgap group III-Nitride materials have several advantages, which include a large bandgap, a high breakdown field, and a high electron drift velocity. From this group, GaN drew attention recently, since it exhibits favorable velocity-field characteristics [3] and can offer higher operation frequency than GaAs [4]. In recent work [5], bias oscillations could be observed for a GaN Gunn diode realized on a  $n^+$ -GaN substrate. A material with even more favorable velocity-field characteristics is InN. This material offers both about fifteen times higher NDM as well as about six times higher low-field mobility than GaN. However, InN did not attract much interest so far, most probably due to its narrower bandgap than

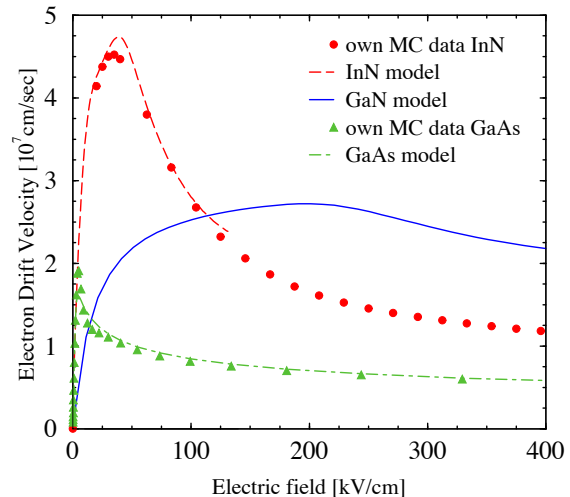


Figure 1: Electron drift velocity vs. electric field.

that of GaAs. In this work, we evaluate and compare the performance of GaN and InN devices.

## 2 PHYSICAL MODELING

Novel emerging devices based on the Nitride material system require physics-based models to properly describe their electrical and thermal behavior. Basic parameter for expressing the currents in a semiconductor device is the carrier mobility. In recent work we proposed new mobility models for electrons suitable for the drift-diffusion and the hydrodynamic transport models [6,7]. These models were calibrated against Monte Carlo simulation results and experimental data for GaN, AlN, and InN [8]. Specific effects are accounted for, such as the negative differential mobility observed at high electric fields (see Fig. 1), which is a reason for occurring of Gunn oscillations [9]. The models and the model parameters values were implemented in our two-dimensional device/circuit simulator [10] and were verified against measured transistor characteristics and allow simulation of various III-Nitride semiconductor devices.

Table 1: Physical parameters and design constraints for GaN, InN, and GaAs devices.

| Material                                       | GaN                  | InN                  | GaAs               |
|--|----------------------|----------------------|--------------------|
| $\mu_0$ [ $\text{cm}^2/\text{Vs}$ ]            | 1600                 | 10200                | 8000               |
| $D_s$ [ $\text{cm}^2/\text{s}$ ]               | 40                   | 270                  | 180                |
| $\epsilon_r$                                   | 8.9                  | 11                   | 12.9               |
| $\nu$ [ $\text{cm}/\text{s}$ ]                 | $2.5 \times 10^7$    | $4.8 \times 10^7$    | $1.5 \times 10^7$  |
| $F_{\text{th}}$ [ $\text{kV}/\text{cm}$ ]      | 200                  | 40                   | 4                  |
| $\mu_{\text{NDR}}$ [ $\text{cm}^2/\text{Vs}$ ] | 40                   | 650                  | 1000               |
| $N \times L$ [ $\text{cm}^{-2}$ ]              | $1.6 \times 10^{13}$ | $2.1 \times 10^{12}$ | $3 \times 10^{15}$ |
| $N_{\text{crit}}$ [ $\text{cm}^{-3}$ ]         | $4 \times 10^{18}$   | $5 \times 10^{17}$   | $5 \times 10^{11}$ |

### 3 DESIGN CRITERIA

Gunn oscillators typically employ of n-i-n diode structures, which must fulfill specific design criteria [9]. One of them is the so-called Kroemer criterion:

$$N_0 \times L > \frac{3\epsilon_r\epsilon_0\nu}{q|\mu_{\text{NDR}}|}. \quad (1)$$

Here,  $N_0$  denotes the doping concentration in the intrinsic layer,  $L$  is its length,  $\epsilon_r\epsilon_0$  is the material's dielectric permittivity,  $\nu$  is the velocity of the Gunn domain, and  $\mu_{\text{NDR}}$  is the negative differential mobility. This criterion must be fulfilled in order Gunn domains to occur. Another condition must be fulfilled to secure stable amplification regime:

$$N_0 < N_{\text{crit}} = \frac{\epsilon_r\epsilon_0\mu_0 F_{\text{th}}^2}{qD_s} \quad (2)$$

$\mu_0$  is the low-field mobility,  $F_{\text{th}}$  is the threshold field for inter-valley transfer, and  $D_s$  is diffusion coefficient. The parameter values are summarized in Table 1 together with the resulting values for  $N_{\text{crit}}$  and  $N_0 \times L$ . As can be seen in Table 1 the higher  $F_{\text{th}}$  leads to some orders of magnitude higher  $N_{\text{crit}}$ . On the other hand, the lower limit for the  $N_0 \times L$  product is higher for Nitrides due to higher electron velocity and lower NDM.

The simulated devices have a homogeneously-doped active layer of  $1 \mu\text{m}$  or  $3 \mu\text{m}$  length and two highly-doped ( $10^{19} \text{cm}^{-3}$ ) regions of  $0.1 \mu\text{m}$  each. The donor concentration in the active layer is chosen so that the critical doping concentration for GaN [11] and InN is not exceeded for both devices. In this way, the formation of static Gunn domains in the anode is avoided and the device's operation in the NDM regime is ensured.

### 4 SIMULATION RESULTS

In order to obtain much higher efficiency, the device is placed into a microwave LCR-cavity as depicted in Fig. 2. This is a parallel resonant circuit which needs to be matched for each geometry, doping and material (see Table 2).

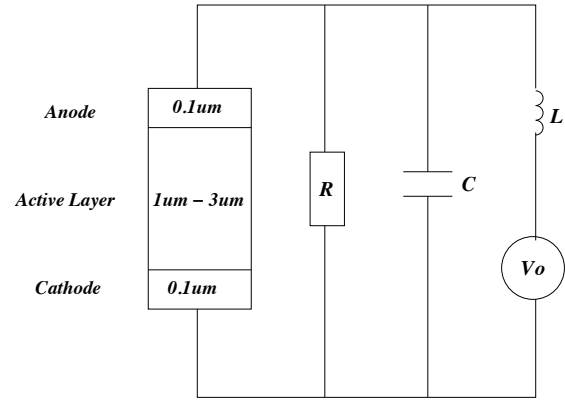


Figure 2: Schematic of the Gunn diode and resonant cavity.

As the first step, our model was verified against results from [4] for a GaN Gunn diode with  $L = 3 \mu\text{m}$ ,  $N_0 = 10^{17} \text{cm}^{-3}$ , and device area of  $2000 \mu\text{m}^2$ . Using the same LCR-circuit identical results were obtained (see Table 2). Fig. 3 shows snapshots of the evolution of the electron concentrations in the GaN diode, which are taken in subsequent time instances with interval of 1 ps. As can be seen in the Fig 3, stable domains of high electron concentration occur, which lead to inhomogeneities in the electric field distribution, illustrated in Fig. 4. Accordingly, the electron concentration and electric field for InN diode is depicted in Fig. 5 and Fig. 6. As the devices are biased over the threshold field  $F_{\text{th}}$  ( $\approx 200 \text{kV}/\text{cm}$  for GaN against  $\approx 40 \text{kV}/\text{cm}$  for InN), the formation of a first stable Gunn domain near the cathode at  $t_0$  is observed. At the next time instances, the Gunn domains propagate in the direction of the anode, where they are annihilated. The formation of Gunn domains will continue as long as the mean electric field is above the threshold field  $F_{\text{th}}$ . A comparison between Fig. 3 and Fig. 5 shows that the Gunn domains propagate much faster in the InN diode. This is due to the considerably higher electron velocity in this material.

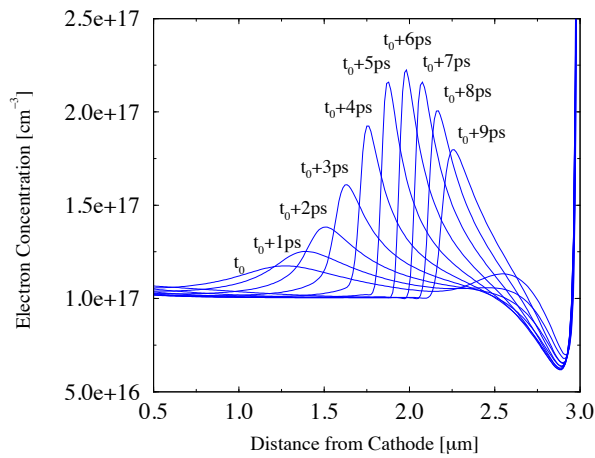


Figure 3: Electron domains in the GaN diode with time step  $\Delta t = 1$  ps ( $t_0=40$  ps).

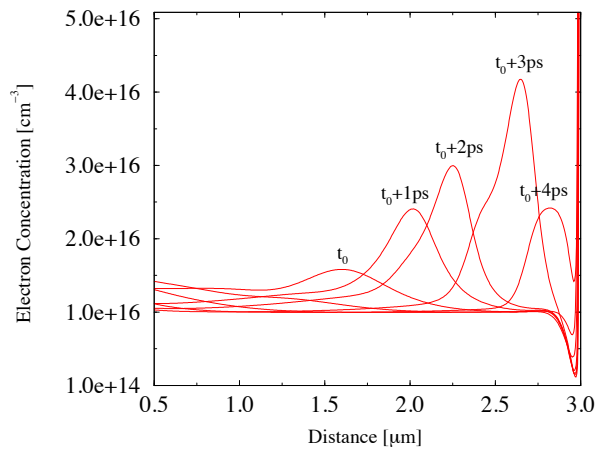


Figure 5: Electron domains in the InN diode with time step  $\Delta t = 1$  ps ( $t_0=40$  ps).

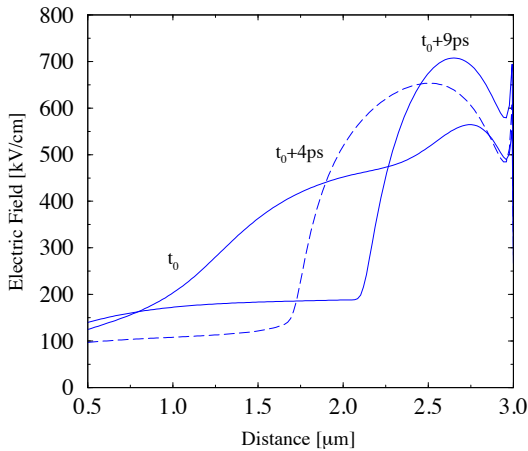


Figure 4: Electric field in the GaN diode at time steps  $t = 4$  ps, 9 ps ( $t_0=40$  ps).

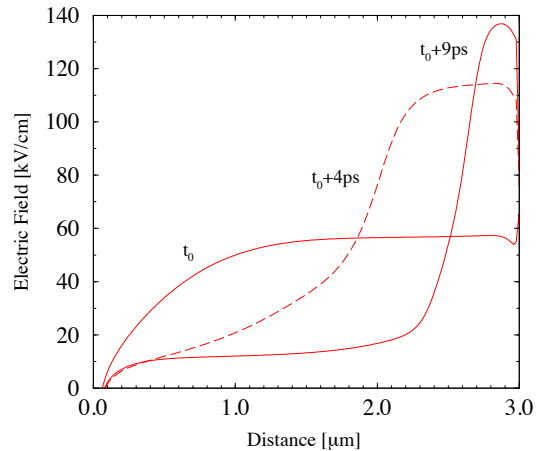


Figure 6: Electric field in the InN diode at time steps  $t = 4$  ps, 9 ps ( $t_0=40$  ps).

Using the mixed-mode device/circuit transient hydrodynamic simulation the output waveforms of the devices are obtained (see e.g. Fig. 7 and Fig. 8). These waveforms are used to extract the oscillation frequency and the output power. Input parameters and the corresponding simulation results for the  $3 \mu\text{m}$  devices of GaN, InN, and GaAs are summarized in Table 2.

Using the same simulation approach, the performance of GaN, InN and GaAs devices with an active length of  $1 \mu\text{m}$  was investigated. For the geometry given and taking into consideration the design constraints, the doping concentrations, the bias voltage, and the LCR-cavity parameters were tuned for maximal device performance (see Table 3).

The simulation results predict superior high-frequency and power performance for both Nitride compounds compared to

GaAs. While GaN significantly outperforms other materials in terms of power density at frequencies below 200 GHz, InN shows comparable performance at about 200 GHz.

## 5 CONCLUSION

In this paper, we present simulation results of Nitride-based Gunn diodes. Our investigations show that both GaN and InN outperform GaAs in microwave applications. In addition, Nitride-based Gunn diodes are suitable for integration in upcoming Nitride technologies. Although GaN has attracted much interest recently, InN also offers potential advantages. Due to higher NDM, InN devices would easier fulfill the criteria for operation in the Gunn-regime, which gives them a good chance of experimental realization.

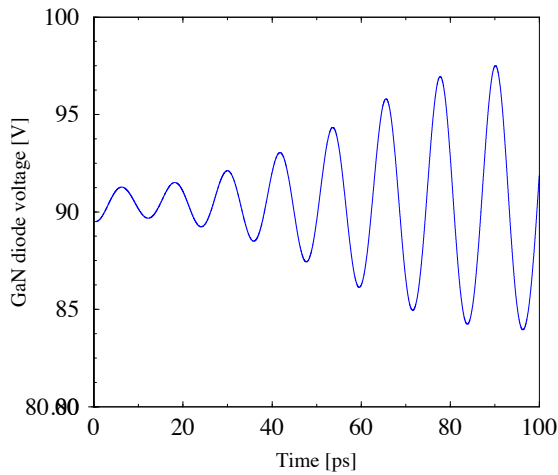


Figure 7: Voltage waveforms for the 3  $\mu\text{m}$  GaN diode.

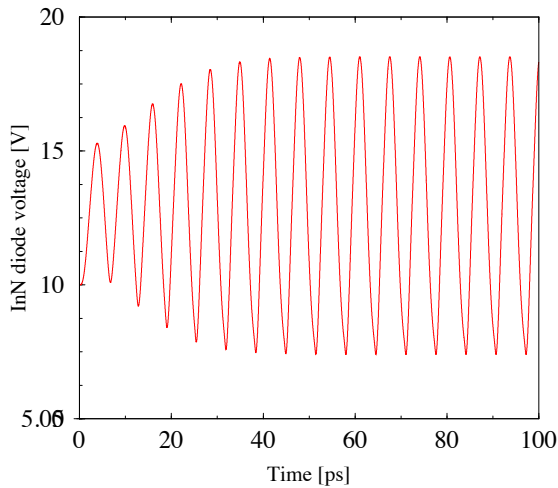


Figure 8: Voltage waveforms for the 3  $\mu\text{m}$  InN diode.

## 6 ACKNOWLEDGEMENTS

Support by the Austrian Science Funds FWF, START Project No.Y247-N13 is acknowledged.

## REFERENCES

- [1] S.J.J. Teng and R.E. Goldwasser, “High-Performance Second-Harmonic Operation W-Band GaAs Gunn Diodes”, *IEEE Elec. Dev. Lett.*, vol. 10, no. 9, pp. 412–414, Sep. 1989.
- [2] C. Li, A. Khalid, N. Pilgrim, M.C. Holland, G.Dunn and D.S.R. Cumming, “Novel Planar Gunn Diode Operating in Fundamental Mode up to 158GHz”, *J. Phys.: Conf. Ser.*, no. 193, 2009.

Table 2: Device and setup parameters for the 3  $\mu\text{m}$  devices.

| Material                         | GaN*            | GaN             | InN             | GaAs      |
|----------------------------------|-----------------|-----------------|-----------------|-----------|
| $N_0$ [ $\text{cm}^{-3}$ ]       | $10^{17}$       | $10^{16}$       | $10^{16}$       | $10^{16}$ |
| $V_0$ [V]                        | 90              | 90              | 13              | 2         |
| $L$ [pH]                         | 17.5            | 17.5            | 8               | 0.1       |
| $C$ [pF]                         | 0.1             | 0.1             | 0.01            | 25        |
| $R$ [ $\Omega$ ]                 | 50              | 50              | 90              | 50        |
| $f$ [GHz]                        | 70              | 85              | 150             | 97        |
| Power [ $\text{W}/\text{cm}^2$ ] | $3 \times 10^5$ | $3 \times 10^4$ | $3 \times 10^2$ | 1.6       |

Table 3: Device and setup parameters for the 1  $\mu\text{m}$  devices.

| Material                         | GaN                | InN                | GaAs      |
|----------------------------------|--------------------|--------------------|-----------|
| $N_0$ [ $\text{cm}^{-3}$ ]       | $5 \times 10^{17}$ | $5 \times 10^{17}$ | $10^{16}$ |
| $V_0$ [V]                        | 45                 | 8                  | 2         |
| $L$ [pH]                         | 1.0                | 0.08               | 0.1       |
| $C$ [pF]                         | 0.2                | 5.0                | 25        |
| $R$ [ $\Omega$ ]                 | 150                | 150                | 150       |
| $f$ [GHz]                        | 200                | 213                | 103       |
| Power [ $\text{W}/\text{cm}^2$ ] | $6 \times 10^4$    | $4.5 \times 10^4$  | 1.0       |

- [3] R.P. Joshi, S. Viswanadha, P. Shah, and R.D. del Rosario, “Monte Carlo Analysis of GaN-Based Gunn Oscillators for Microwave Power Generation”, *J.Appl.Phys.*, vol. 93, no. 8, pp. 4836–4842, Apr. 2003.
- [4] E. Alekseev and D. Pavlidis, “GaN Gunn Diodes for THz Signal Generation”, in *Tech. Dig. IEEE MTT-S Intl. Microw. Symp.*, vol. 3, pp. 1905–1908, Jun. 2000.
- [5] O. Yilmazoglu, K. Mutamba, D. Pavlidis and T. Karaduman, “First Observation of Bias Oscillations in GaN Gunn Diodes on GaN Substrate”, *IEEE Trans. Elec. Dev.*, vol. 55, no. 6, pp. 1563–1567, Jun. 2008.
- [6] S. Vitanov, V. Palankovski, S. Maroldt, and R. Quay, “High-Temperature Modeling of AlGaIn/GaN HEMTs”, *Solid-State Electron.*, vol. 54, no. 10, pp. 1105–1112, Oct. 2010.
- [7] S. Vitanov, V. Palankovski, and S. Selberherr, “Hydrodynamic Models for GaN-Based HEMTs”, in *Proc. Europ. Solid-State Dev. Res. Conf. Fringe Poster Session*, Sep. 2010.
- [8] S. Vitanov, V. Palankovski, “Monte Carlo Study of Electron Transport of InN”, *Springer Proc. in Physics*, vol. 119, pp. 97–100, Springer, Dordrecht, 2008.
- [9] M. Shur, “GaAs Devices and Circuits”, Plenum Press, New York and London, 1987.
- [10] Minimos-NT Device and Circuit Simulator, User’s Guide, <http://www.iue.tuwien.ac.at/mmnt>.
- [11] T.G. Ruttan, “High Frequency Gunn Oscillators”, *IEEE Trans. on MTT*, vol. 22, no. 2, pp.142–144, Feb. 1974.